Nov 13th, 12:00 AM

Strength of Biaxially Compressed Perforated Plates

Rangachari Narayanan

Fong-Yen Chow

Seventh International Specialty Conference on Cold-Formed Steel Structures
St. Louis, Missouri, U.S.A., November 13-14, 1984

STRENGTH OF BIAXIALLY COMPRESSED PERFORATED PLATES

by

Rangachari NARAYANAN and Fong-Yen CHOW*

SUMMARY

An approximate method of predicting the post-buckling behaviour and the ultimate carrying capacity of perforated plates under biaxial compression is presented. The theory is based on a mechanism solution, used in conjunction with an elastic loading path derived from the energy method. Comparisons with test results have shown that satisfactory predictions of peak strengths and good approximations of the loading and unloading paths for simply supported plates containing square and circular cutouts have been obtained by the theory suggested.

INTRODUCTION

Plate panels used in many structural applications are often subjected to both longitudinal and transverse in-plane loading. Frequently these are provided with openings to facilitate access for services, inspection and maintenance.

Only a few investigators [1,3,5,7,8,10,16,21,24] have concerned themselves with biaxially loaded plates and the authors could not locate any published work on experimental or theoretical investigations into the behaviour of perforated plates under biaxial loading; in view of this, experimental and theoretical investigations on this subject were undertaken and this paper presents the results of these studies.

In view of the complexities in analysing perforated plates, the theoretical analysis developed in this paper is approximate and is obtained by considering the elastic post-buckled behaviour of the plate as well as its rigid plastic unloading characteristic in the collapse state. The ultimate load is approximately estimated from the point of intersection of the elastic loading curve and the plastic unloading curve (see Fig. 1).

SCOPE OF THE INVESTIGATIONS

A series of biaxial compression tests were carried out on perforated plates containing centrally located circular and square openings, in order to obtain data on the buckling and post-buckling behaviour of these plates. Only square plates were tested and the sizes of openings were limited to a maximum diameter and side equal to half the width of the plate. The following aspects of the problem were covered by the study :

(a) The longitudinal edge strain was kept equal to the transverse edge strain, i.e. the strain ratio was maintained at a single value (of 1).

(b) Both circular and square holes were introduced and their influence on the buckling and ultimate capacity of the plates was studied.

---

* University College, Cardiff, U.K.

(c) The effect of holes on plates having various $\frac{\text{width}}{\text{thickness}}$ ratios $(\frac{a}{t})$ was examined.

The tests are classified into three groups and the details of the tested plates are presented in Table 1. Group 1 tests were aimed at studying the effect of varying the size of the circular holes upon the strengths of the plate; a single value of plate slenderness ($a/t \simeq 77$) was employed in this group and the sizes of the holes ranged from 0 to 0.5a.

Group 2 tests were aimed at ascertaining the influence of plate slenderness (a/t), on the behaviour of perforated plates. The tests were carried out using two hole sizes of 0.291a and 0.465a , and the values of plate slenderness (a/t) were changed by varying the plate thicknesses; three (a/t) values viz. 42,53 and 88 were employed.

Group 3 tests were similar to group 1 tests, with the difference that the holes were square. The effect of the shape of the hole could be ascertained by comparing the results of this group of tests with group 1 tests.

It will be observed that all the tests reported in this paper were carried out on small scale models; an extensive series of tests carried out at Cardiff and elsewhere, on the buckling and post buckling characteristics of plates have established that small scale models can be employed to simulate the behaviour of larger prototypes, without any loss of accuracy [9,12,15,22]. The small scale models have the added advantage of economy in fabrication and testing costs. It was therefore possible to test at least two models for each of the variables studied, to ascertain the repeatability of the tests.

EXPERIMENTATION

The object of the experiments reported in this paper is to subject a number of plate specimens detailed above, to uniform edge strains and to study the load-deflection behaviour extending to well beyond the peak load. As detailed in Tables 1 and 2, some 15 tests were carried out on plates having various slenderness (a/t) values.

A purpose built rig was fabricated with sufficient stiffness to test mild steel plates under biaxial loading. A photograph of the test rig is shown in Fig. 2. It is capable of applying a maximum load of 90 kN in the longitudinal and transverse directions and testing plate specimens up to 300mm x 300mm. The rig is desk-mounted and self-contained and no strong floor or supporting frame work is necessary. It is hand operated and is suitable for testing small-scale models in the laboratory. A full description of the test rig is given in reference 4.

The loads were applied by positioning hydraulic jacks at the desired locations and operating the pump; the applied loads were measured by load cells placed between the jacks and the cross arms at the edges of the plate under test. Out-of-plane displacements were measured by setting transducer gauges directly over the plate. The load cells and the transducers were connected to Gemini digital voltmeters and the loads were measured to an accuracy of 0.02 kN and the displacements to 0.01mm.

The initial imperfections of the plate were measured by moving a transducer gauge supported on a transverse bar and connected to an x-y plotter. Measurements were taken at several locations along the length of the plate. The dimensions of the tested plates and the maximum initial imperfections are reported in Table 1. Off-cuts from the material used in making the test specimens were tested for yield strength, and these are also reported in the table.

DETERMINATION OF BUCKLING LOADS

The experimental buckling loads are obtained by the inflection-point method |19|; the "inflection point" is defined as the load corresponding to the point where the rate of change of slope of the load-deflection curve is a minimum. Its determination from experimental data is less dependent on individual judgement than some of the other methods available; these points on the load deflection curves are obtained by applying least-square curve-fitting techniques to the experimental data. Good correlation between theoretical buckling loads and the values determined by this method have been obtained by Narayanan and Chow |13, 14| for perforated plates subjected to shear loading and uniaxial compression.

The theoretical elastic critical stress for a simply supported plate subjected to biaxial compression is given by |20| :

$$\sigma^{b}_{cr} = \left(\sigma_x \frac{b}{a} + \sigma_y \frac{a}{b}\right)^{c} = K^{o}_{b} \frac{\pi^2 E}{12(1-\nu^2)} \left(\frac{t}{b}\right)^2 \qquad (1)$$

where K^{o}_{b} is the buckling coefficient given by $\left(\frac{b}{a} + \frac{a}{b}\right)^2$ for an unperforated plate

The elastic critical stress appropriate to a similar plate containing a rectangular or circular perforation can be expressed by an equation similar to (1) :

$$\sigma^{h}_{cr} = K_b \frac{\pi^2 E}{12(1-\nu^2)} \left(\frac{t}{b}\right)^2 \qquad (1a)$$

where K_b is the reduced value of buckling coefficient due to the presence of the opening.

Values of K_b obtained experimentally are compared with the corresponding computed values using a finite element method suggested by Sabir and Chow |18|. The measured values are presented in Table 2.

ELASTIC POST BUCKLING BEHAVIOUR OF BIAXIALLY LOADED PERFORATED PLATES

The theoretical elastic analysis developed by Narayanan et al |16| will be used for tracing the elastic loading behaviour. They have assumed that the initial surface of the plate before any loads are applied is given by :

$$w_o = \delta_o \sin \frac{\pi x}{a} \cdot \sin \frac{\pi y}{b} \qquad (2)$$

where

w_o = initial deflection function

δ_o = the maximum initial imperfection at the centre of plate

a,b = sides of an approximately square plate

Under the influence of loading, the surface of the plate changes to

$$w = \delta \sin \frac{\pi x}{a} \sin \frac{\pi y}{b} .$$

Using the Energy Method, they have derived the following equations for evaluating the stress distribution across the plate when subjected to biaxial compression in the post-buckled stage; the approximate stress-strain relationship is given by :

$$\beta \cdot d\varepsilon_x + \frac{1}{\beta} d\varepsilon_y = \left(\sigma_x \frac{b}{a} + \sigma_y \frac{a}{b}\right)^{c} \frac{dm}{m^2 E} + \frac{3\pi^2}{8} \left(\frac{\delta_o}{b}\right)^2 \left(\frac{\beta^4 + 1}{\beta}\right) m \, dm$$

$$- \frac{\nu}{E} \{\frac{\beta}{a} \int_o^a d\sigma_{ya}\, dx + \frac{1}{\beta b} \int_o^b d\sigma_{xa}\, dy\} \qquad (3)$$

where $\beta = \frac{b}{a}$ and m = magnification ratio for plate deflection = $\frac{\delta}{\delta_o}$

$\left(\sigma_x \frac{b}{a} + \sigma_y \frac{a}{b}\right)^c$ is the combination stresses in an unperforated plate under biaxial loading, at the elastic critical state.

$d\sigma_{xa}$ and $d\sigma_{ya}$ in eq. (3) were obtained from :

$$d\sigma_{xa} = E\{d\varepsilon_x - \frac{\pi^2 \delta_o^2\, mdm}{4a^2} + \frac{\nu}{aE} \int_o^a d\sigma_{ya}\, dx\}$$
$$d\sigma_{ya} = E\{d\varepsilon_y - \frac{\pi^2 \delta_o^2\, mdm}{4b^2} + \frac{\nu}{bE} \int_o^b d\sigma_{xa}\, dy\} \qquad (4)$$

The stresses in the post-buckling stage are computed from :

$$\sigma_x = \sigma_{xa} + \frac{\pi^2 E(\delta^2 - \delta_o^2)}{8a^2} \cos \frac{2\pi y}{b} = \sigma_{xa} + \sigma_{xy}$$
$$\sigma_y = \sigma_{ya} + \frac{\pi^2 E(\delta^2 - \delta_o^2)}{8b^2} \cos \frac{2\pi x}{a} = \sigma_{ya} + \sigma_{yx} \qquad (5)$$

The above equations can be solved by numerical integration to obtain the values of σ_x and σ_y corresponding to any combination of axial strains ($\varepsilon_x/\varepsilon_y$) .

An approximate relationship for the perforated plate can be suggested in an analogous manner. Firstly, the elastic critical stress of the unperforated plate in equation (3) can be replaced by the elastic critical stress of the perforated plate σ_{cr}^h obtained by the finite element method |18|.

Ritchie and Rhodes |17|, have reported on the post buckled behaviour of axially compressed perforated plates. They have suggested that the influence of the hole in a buckled plate may be approximated as follows : It is assumed that the compressive stresses released by the introduction of a hole in the perforated plate may be redistributed over the remaining width of the plate which carry stresses.

In this paper, this concept has been extended to compute the elastic stress distribution across the hole in the post-buckled stage when the plate is subjected to biaxial compression. The typical stress distribution across a hole is shown in Fig. 3.

The elastic load displacement relationship is obtained from equations (3) to (5) and used to obtain the "loading" curve of the type shown in Fig. 1.

MECHANISM SOLUTION

Several investigators |6,23| have obtained mechanism type solutions to model rigid plastic unloading lines for simply supported plates subjected to uniaxial compression. The rigid plastic mechanism solution was also employed by Narayanan and Chow |14| to obtain the ultimate capacity of the uniaxially loaded perforated plates. A similar method is formulated in this paper to study the ultimate capacity of an approximately square perforated plate, subjected to biaxial compression.

A study of the failure pattern observed in the tests (see photographs in Fig. 4) suggests a relatively simple model of collapse mechanism for perforated plates with square and circular cutouts. The collapse mechanism is approximated as shown in Fig. 5 and consists of four yield lines which start from the four corners (A,B,E,F) and end at the hole boundary (C,D,H,I), with rigid quadrantal segments between the yield lines. The edges of the plate and the yield lines are the axes of rotation for the rigid regions of the plate, i.e. the rotation of the yield lines is the deformation of the plate.

A simplified form of Von Mises Yield criterion is used and is given by :

$$\frac{M}{M_p} + \left(\frac{P}{P_p}\right)^2 + \left(\frac{S}{S_p}\right)^2 = 1 \qquad (6)$$

where the shear force (S) , the membrane force (P) , and the moment per unit length (M) of the yield line are given by [11]

$$S = \tau.t \; ; \; P = 2c\sigma \; ; \text{ and } \; M = \frac{\sigma t^2}{4}\left|1 - \left(\frac{2c}{t}\right)^2\right| \qquad (7)$$

where 2c = depth of the plate in compression (see Fig. 6)

and $$M_p = \frac{\sigma_{ys}.t^2}{4} \; , \; P_p = \sigma_{ys}.t \text{ and } S_p = \frac{\sigma_{ys}.t}{\sqrt{3}} \qquad (8)$$

The mechanism shown in Fig. 5(a) for a plate containing a square cutout will now be considered. Considering a rectangular element Q having sides ∂x and ∂y as shown in Figs. 5(a) and 7(a), p_x and p_y are the contributions of membrane forces per unit length along the yield lines. p_x is due to P_{xh} and p_y is due to P_{yh} and $P = p_x + p_y$. P_{1x} is the equivalent uniformly distributed load per unit length, acting on C'D' and P_{1y} is the equivalent uniformly distributed load per unit length, acting on C"H" . P_{2x} is the nonuniform load per unit length acting on AC' and P_{2y} is the nonuniform load per unit length acting on AC" (see Fig. 7(b)).

Resolving the forces in the x and y directions, we obtain

$$\int_0^{\ell'} P_{2x}\, dy + \int_0^{\frac{1}{2}b'} P_{1x}\, dy = \int_0^{\ell' \operatorname{cosec}\alpha} (p_y + p_x) \sin d\eta + \int_0^{\ell' \operatorname{cosec}\alpha} S \cos\alpha \, d\eta \qquad (9)$$

$$\int_0^{\ell_1'} P_{2y}\, dx + \int_0^{\frac{1}{2}a'} P_{1y}\, dx = \int_0^{\ell' \operatorname{cosec}\alpha} (p_y + p_x)\cos\alpha \, d\eta - \int_0^{\ell' \operatorname{cosec}\alpha} S \sin\alpha \, d\eta \qquad (10)$$

The moment per unit length of the yield line M is composed of two components M_x and M_y ; let the component of the plastic moment caused by P_{yh} be M_y and that due to P_{xh} be M_x , so that $M = M_x + M_y$.

Moment equilibrium about the inclined yield line is obtained as :

$$\int_0^{\ell'} P_{2x}\, y \frac{\delta'}{\ell'}\, dy + P_{1x} \frac{b'}{2} \frac{\delta'}{2} + \int_0^{\ell_1'} P_{2y}\, x \frac{\delta'}{\ell_1'}\, dx + P_{1y} \frac{a'}{2} \frac{\delta'}{2}$$

$$= \int_0^{\ell' \operatorname{cosec}\alpha} M_x \operatorname{cosec}\alpha \, d\eta + \int_0^{\ell' \operatorname{cosec}\alpha} M_y \sec\alpha \, d\eta \qquad (11)$$

where $\ell' = \frac{1}{2}(b-b')$ and $\ell_1' = \frac{1}{2}(a-a')$

Taking $\gamma' = P'_y/P'_x$, where $P'_y = P_{2y} + (a'/a-a')P_{1y}$ and $P'_x = P_{2x} + (b'/b-b')P_{1x}$, equations (6), (9), (10) and (11) may be solved numerically for P'_x/P_p for any given ratio of γ'. The unknown quantity of (M_y/M_x) may be obtained by trial and error to satisfy equation (6). The total load P_{xh} carried by this mechanism when normalized by squash load ($P_{sq} = \sigma_{ys}.b.t$) is given by

$$\frac{P_{xh}}{P_{sq}} = \frac{2}{b}\left(\int_0^{\ell'} \frac{P_{2x}}{P_p}\,dy + \int_0^{\frac{b'}{2}} \frac{P_{1x}}{P_p}\,dy\right) \qquad (12)$$

For the purpose of illustration, the case of a square plate with a square hole is considered with the longitudinal load P_{xh} equal to transverse load P_{yh}. For an inclined angle α equal to 45°, equation (12) becomes

$$\frac{P_{xh}}{P_{sq}} = \frac{b-b'}{b}\left(\sqrt{1 + \left(\frac{2\delta'}{t}\right)^2} + \frac{1}{\frac{2\delta'}{t}}\ln\left(\frac{2\delta'}{t} + \sqrt{1 + \left(\frac{2\delta'}{t}\right)^2}\right) - \frac{2\delta'}{t}\right) \qquad (13)$$

Equation (13) gives the load deflection relationship for a square plate with a square cutout. The equation can also be used for circular cutout with diameter d, by replacing the width of the cutout b' of equation (13) by 0.707 d .

EXPERIMENTAL RESULTS

Experimentally observed collapse loads are compared with the theoretically predicted values obtained from the intersection of the plastic unloading line and the elastic loading curve using the measured values of imperfections. The results of the measured buckling loads and the theoretical and observed failure loads are presented in Table 2.

The two ultimate loads are presented as ratios between the loads at collapse and the corresponding squash loads.

Comparison of Observed Buckling Loads with Theoretical Predictions :

Figure 8 presents a comparison of the buckling coefficients obtained from the experiments with the computed results obtained by the finite element method. Good agreement between the experimental and theoretical buckling coefficients is observed for perforated plates containing both circular and square holes.

Ultimate Capacity of Perforated Plates :

In Table 2, the observed ultimate loads are compared with the predicted values using the theory outlined above. A comparison of the experimental and theoretical failure loads shows that the predictions are generally satisfactory. The mean value of the predicted strengths/observed strengths for the 15 tests was 1.046 with a standard deviation of 0.074 ; this shows that the proposed theory predicts the strength of the perforated plates to a sufficient degree of accuracy, if slightly unconservatively.

Typical experimental load deflection relationships are plotted in Fig. 9 for four plates having a/t values of 77.4 containing circular or square holes. It will be seen that the peak loads are closely predicted from the method described in this paper and the observed loading and unloading curves are close to the theoretical curves, which are also plotted in the same figure.

Observations from tests in groups 1 and 3 suggest that there is a drop in strength with increasing hole sizes corresponding to the loss of stiffness of the plate due to the presence of holes. However, there is little difference

between the ultimate strengths of the plates containing circular and square cut-outs.

A study of group 2 tests shows that no discernable pattern of the drop of strength with increasing a/t ratio was discovered; this applies for all hole diameters studied.

DESIGN CURVES

Design curves using the theory outlined in this paper are given in Fig. 10 and are suitable for assessing the ultimate strengths of square plates containing circular and square perforations. In deriving these curves, the initial imperfections used are in accordance with the following formula which is regarded as realistic for practical plated structures [2].

$$\frac{\delta_o}{t} = 0.145 \frac{a}{t} \sqrt{\frac{\sigma_{ys}}{E}} \qquad (14)$$

These curves can be readily used by designers for square plates; similar curves can be readily plotted for rectangular plates with central holes, using the theory outlined in the paper.

CONCLUSIONS

A method of evaluating the ultimate capacity of simply supported rectangular perforated plates under biaxial compression is suggested in this paper. The method is based on the elastic loading behaviour and the plastic unloading characteristic of the plate.

Tests carried out on a specially fabricated rig shows that the observed collapse loads are close to the predicted ultimate capacity of the plates; predictions obtained are slightly unconservative.

For the range of hole sizes considered, the loss in strength due to the introduction of the opening is rapid when the plate slenderness (a/t) is smaller than 50 ; for higher values of a/t , the loss in strength is gradually reduced.

Design curves which can be used to assess the ultimate strength of square plates with square and circular openings have been proposed and these can be used directly; similar curves can be readily obtained for rectangular plates using the method outlined in the paper.

APPENDIX I : REFERENCES

1. BECKER, H. "Instability strength of polyaxially loaded plates and relation to design". Steel Plated Structures, (edited by Dowling, P.J. et al), Crosby Lockwood Staples, London 1977, pp. 559-580.

2. BRITISH STANDARDS INSTITUTION: BS 5400 PART 3 1982: Code of Practice for the Design of Steel Bridges, British Standards Institution, London, 1982.

3. BECKER, H., GOLDMAN, R. and PAZERYCKI, J. "Compressive strength of ship hull girders. Part 1 Unstiffened Plates". Ship Structure Committee Report SSC 217, 1970.

4. CHOW, F.Y. "Plates under axial compression and shear". Ph.D. Thesis, University of Wales, 1983.

5. COOMBS, M.L. "Aspect of the elasto-plastic behaviour of biaxially loaded plates". M.Sc. Thesis, University of London, 1975.

6. DAVIES, P., KEMP, K.O. and WALKER, A.C. "An analysis of the failure mechanism of an axially loaded simply supported steel plate". Proceedings of The Institution of Civil Engineers, London, Part 2, 59, December 1975, pp. 654-658.

7. DIER, A.F. and DOWLING, P.J. "The strength of plates subjected to biaxial forces". Paper presented at James Harvey Retiral Conference, Strathclyde University, Glasgow, April 1983.

8. DOWLING, P.J., HARDING, J.E. and SLATFORD, J.E. "Strength of ship-plating-plates in biaxial compression". Engineering Structures Laboratories, Imperial College, London, CESLIC Report SP4, November 1979.

9. ELSHARKAWI, K. and WALKER, A.C. "Buckling of multibay stiffened plate panels" Proceedings of the American Society of Civil Engineers, New York, Vol. 106, No. ST8, August 1980, pp. 1695-1715.

10. FRIEZE, P.A., DOWLING, P.J. and HOBBS, R.E. "Ultimate load behaviour of plates in compression". Steel Plated Structures, (edited by Dowling, P.J. et al), Crosby Lockwood Staples, London 1977, pp. 24-50.

11. HORNE, M.R. "Plastic theory of structures". Nelson, 1971.

12. NARAYANAN, R. and ADORISIO, D. "Model studies on plate girders". Journal of Strain Analysis, Institution of Mechanical Engineers, London, Vol. 18, No. 2, 1983, pp. 111-117.

13. NARAYANAN, R. and CHOW, F.Y. "Experiments on perforated plates subjected to shear". To be published in the Journal of Strain Analysis, Institution of Mechanical Engineers, London.

14. NARAYANAN, R. and CHOW, F.Y. "Ultimate capacity of uniaxially compressed perforated plates". To be published in Thin Walled Structures, Applied Science Publishers, London.

15. NARAYANAN, R., DER-AVANESSIAN, N.G.V. and GHANNAM, M.M., "Small scale model tests on perforated webs". The Structural Engineer, London, Vol. 61B, No.3, September 1983. pp. 47-53.

16. NARAYANAN, R., SHANMUGAM, N.E. and CHOW, F.Y. "Compressive strength of biaxially loaded plates". Accepted for publication by the Proceedings of The Institution of Civil Engineers, London.

17. RITCHIE, D. and RHODES, J. "Buckling and post-buckling behaviour of plates with holes". Aeronautical Quarterly, London, November 1975, pp. 281-296.

18. SABIR, A.B. and CHOW, F.Y. "Elastic buckling of flat panels containing circular and square holes". International Conference on Instability and Plastic Collapse of Structures, Manchester, 1983.

19. SCHLACK, A.L. "Elastic stability of pierced square plates". Proceedings of the Society of Experimental Stress Analysis, Vol. 21, June 1964, pp.167-172.

20. TIMOSHENKO, S. and GERE, J. "Theory of Elastic Stability". Second Edition, McGraw-Hill Book Company, New York, 1967.

21. VALSGARD, S. "Ultimate capacity of plates in biaxial compression". Det Norske Veritas Report 78-678, 1978.

22. WALKER, A.C. and DAVIES, P. "An elementary study of non-linear buckling phenomena in stiffened plates". Proceedings of the symposium of Non-linear Behaviour and Technique in Structural Analysis. Report 164 UC, TRRL, Department of the Environment, London, 1975. pp. 19-28.

23. WALKER, A.C. and MURRAY, N.W. "A plastic collapse mechanism for compressed plates". International Association for Bridge and Structural Engineering, Zurich 35, 1975, pp. 217-236.

24. WILLIAMS, D.G. and WALKER, A.K. "Explicit solutions for the design of initially deformed plates subject to compression". Proceedings of The Institution of Civil Engineers, London, Part 2, 59, Dec. 1975, pp. 763-787.

APPENDIX 2 : NOTATION

a,b	dimensions of an approximately square plate
a',b'	dimensions of the rectangular hole
d	diameter of the circular hole
E	modulus of elasticity
K_b	buckling coefficient of the perforated plate
K_b^o	buckling coefficient of an unperforated plate
ℓ'	$\frac{1}{2}(b-b')$
ℓ_1'	$\frac{1}{2}(a-a')$
M	yield moment per unit length of yield line
M_p	moment, M, with zero axial and shearing forces
p	axial force at yield at mid-depth per unit length of yield line
P_{xh}	longitudinal load on the perforated plate
P_{yh}	transverse load on the perforated plate
S	shearing force at yield, per unit length of yield line
S_p	shear force, S, with zero bending and axial forces
t	thickness of plate
w	a function describing the out-of-plane deflection
w_o	a function describing the initial deflection form of the plate
σ_b	normal stress on the yield line
σ_{cr}	biaxial buckling stress of an unperforated plate
σ_{cr}^h	biaxial buckling stress of a perforated plate
σ_x,σ_y	axial stress in the x or y direction
σ_{xa},σ_{ya}	applied stress in the x or y direction
σ_{xy}	induced stress in the x direction due to the action of σ_{ya}
σ_{yx}	induced stress in the y direction due to the action of σ_{xa}
σ_{ys}	yield stress
τ	shear stress on yield line
ν	Poisson's ratio
α	angle of inclination of the yield line
β	$\frac{b}{a}$
δ	maximum value of out-of-plane deflection
δ_o	maximum value of initial plate imperfection
δ'	out of plane deflection at the corner of the hole (at C, D, H and I in Fig. 5a).

TABLE 1

DETAILS OF SPECIMENS WITH CENTRALLY LOCATED HOLES

GROUP	SPECIMEN NO.	a (mm)	t (mm)	$\frac{a}{t}$	d or a' (mm)	$\frac{d}{a}$ or $\frac{a'}{a}$	δ_o (mm)	$\frac{\delta_o}{t}$	σ_{ys} N/mm^2
	CIRCULAR HOLE								
1	BL5	125.0	1.615	77.4	0.0	0.0	0.171	0.106	323.3
	BC2	125.0	1.615	77.4	25.0	0.2	0.195	0.121	323.3
	BC3	125.0	1.615	77.4	37.5	0.3	0.062	0.038	323.3
	BC4	125.0	1.615	77.4	50.0	0.4	0.235	0.146	323.3
	BC5	125.0	1.615	77.4	62.5	0.5	0.104	0.064	323.3
2	BC6	86.0	2.032	42.3	25.0	0.291	0.053	0.026	334.7
	BC7	86.0	1.615	55.3	25.0	0.291	0.155	0.096	323.3
	BC8	86.0	0.972	88.5	25.0	0.291	0.078	0.080	317.6
	BC9	86.0	2.032	42.3	40.0	0.465	0.085	0.042	334.7
	BC10	86.0	1.615	55.3	40.0	0.465	0.148	0.092	323.3
	BC11	86.0	0.972	88.5	40.0	0.465	0.069	0.071	317.6
	SQUARE HOLES								
3	BSQ2	125.0	1.615	77.4	25.0	0.2	0.134	0.083	323.3
	BSQ3	125.0	1.615	77.4	37.5	0.3	0.158	0.098	323.3
	BSQ4	125.0	1.615	77.4	50.0	0.4	0.097	0.060	323.3
	BSQ5	125.0	1.615	77.4	62.0	0.5	0.103	0.064	323.3

TABLE 2

COMPARISON OF TEST RESULTS WITH THEORETICALLY PREDICTED STRENGTHS

GROUP	SPECIMEN NO.	$\frac{a}{t}$	$\frac{d}{a}$ or $\frac{a'}{a}$	Experimental Measured Values: P_{cr} mean (kN)	Experimental Measured Values: K_b mean	Experimental Measured Values: Failure Load (kN)	Experimental Measured Values: Failure Load / Squash load	Predicted strengths $\frac{P_{xh}}{P_{sq}}$	(8) (7)
	1	2	3	4	5	6	7	8	9
	CIRCULAR HOLE								
1	BL5	77.40	0.0	12.235	1.960	27.71	0.425	0.385	0.906
	BC2	77.40	0.2	11.050	1.770	23.45	0.360	0.320	0.889
	BC3	77.40	0.3	10.050	1.610	18.90	0.290	0.298	1.028
	BC4	77.40	0.4	9.805	1.570	15.95	0.245	0.272	1.110
	BC5	77.40	0.5	8.990	1.44	14.35	0.220	0.250	1.136
2	BC6	42.30	0.291	-	-	27.10	0.480	0.470	0.979
	BC7	53.25	0.291	-	-	16.65	0.371	0.390	1.051
	BC8	88.48	0.291	3.50	1.63	7.00	0.259	0.275	1.062
	BC9	42.30	0.465	-	-	20.90	0.370	0.385	1.041
	BC10	53.25	0.465	-	-	15.60	0.348	0.325	0.934
	BC11	88.48	0.465	3.195	1.496	5.65	0.209	0.238	1.139
	SQUARE HOLE								
3	BSQ2	77.40	0.2	10.93	1.751	19.60	0.301	0.310	1.030
	BSQ3	77.40	0.3	10.18	1.630	16.60	0.255	0.275	1.078
	BSQ4	77.40	0.4	9.395	1.504	15.00	0.230	0.240	1.043
	BSQ5	77.40	0.5	10.085	1.615	12.10	0.186	0.210	1.129
							mean		1.046
							standard deviation		0.074

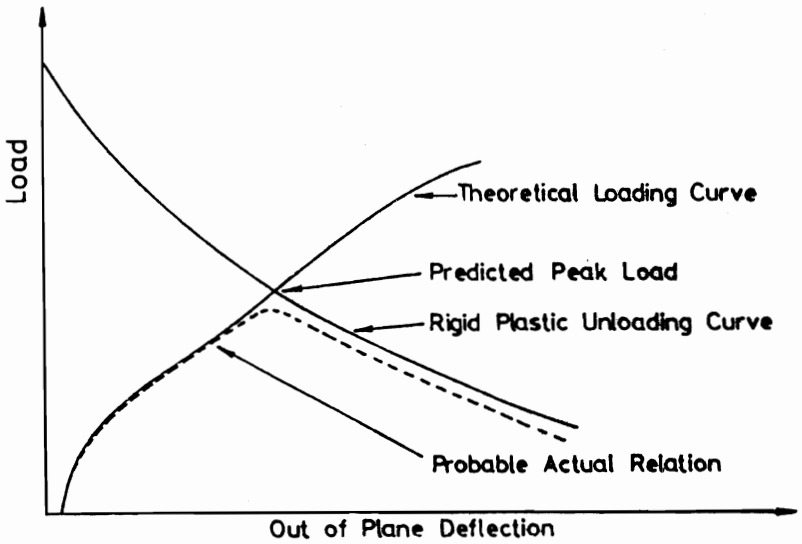
Load
Theoretical Loading Curve
Predicted Peak Load
Rigid Plastic Unloading Curve
Probable Actual Relation
Out of Plane Deflection

Fig. 1

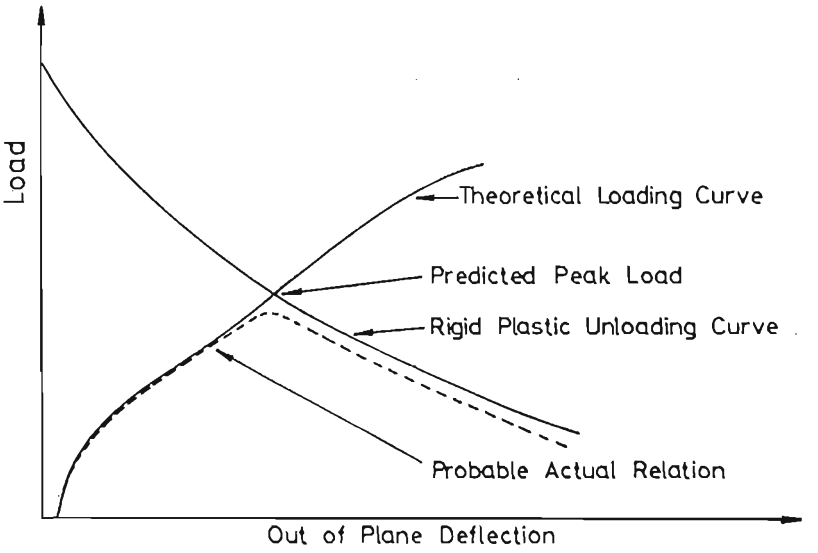

Fig. 1

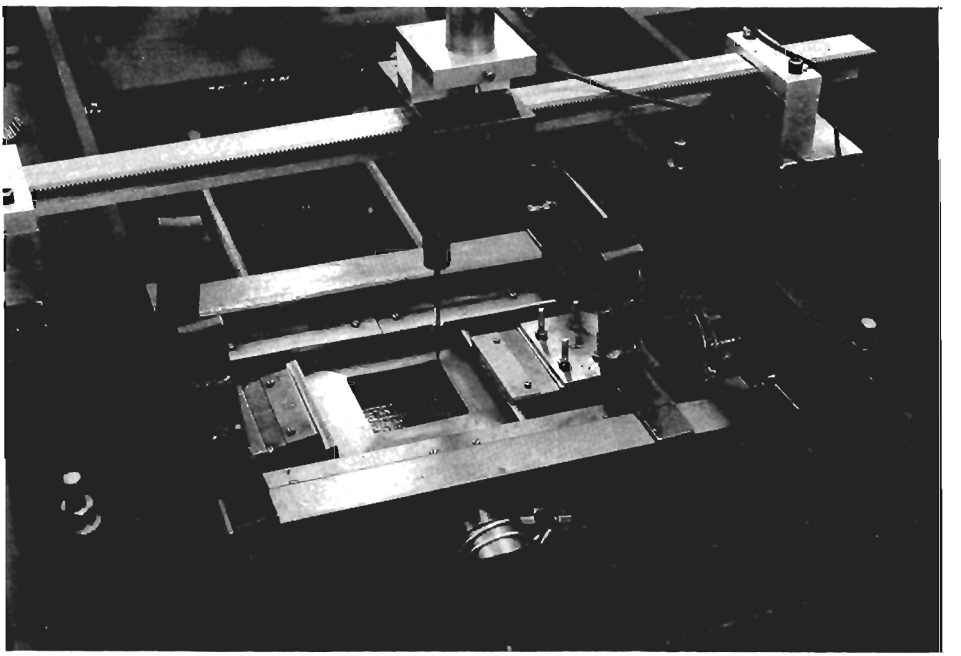

Fig. 2 Test Rig With Specimen Tested To Failure.

$$\frac{a}{t} = 75 \qquad \frac{d}{a} = 0.2 \qquad \frac{\delta_0}{t} = 0.145\,\frac{a}{t}\sqrt{\frac{\sigma_{ys}}{E}}$$

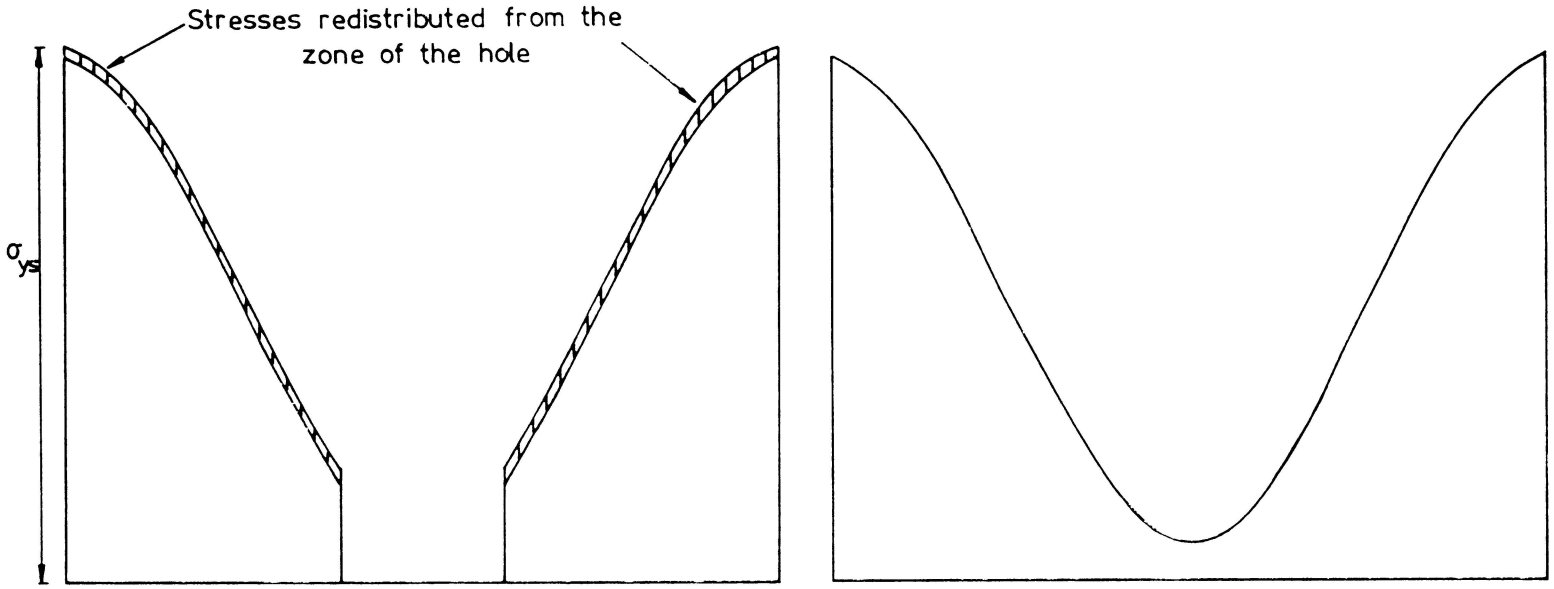

Fig. 3 Typical Stress Distribution

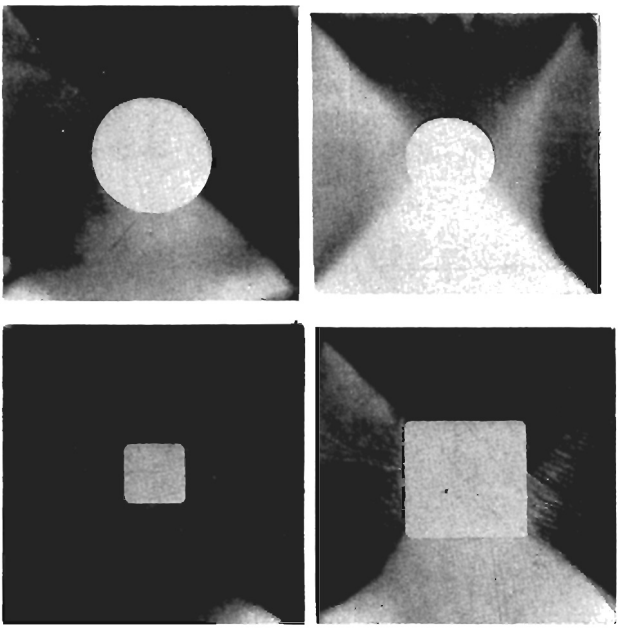

Fig. 4 Plates With Centrally Located Holes Tested To Failure

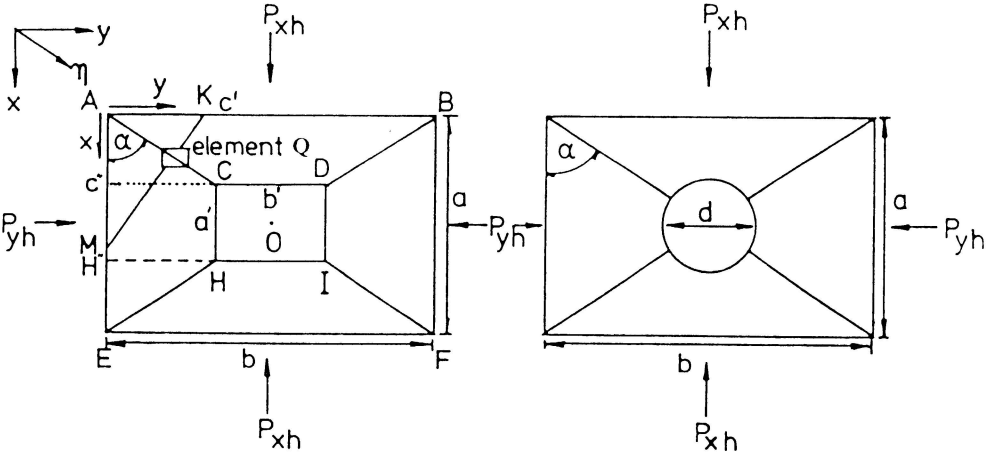

a) geometric model of yield-line pattern of perforated plate with rectangular hole.

b) geometric model of yield-line pattern of perforated plate with circular hole.

Fig. 5

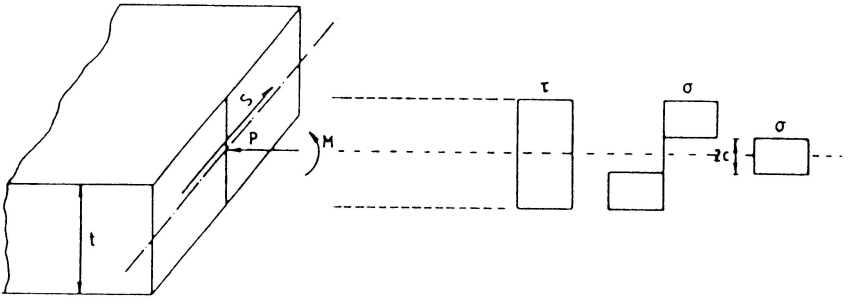

Fig. 6 Section On Yield Line

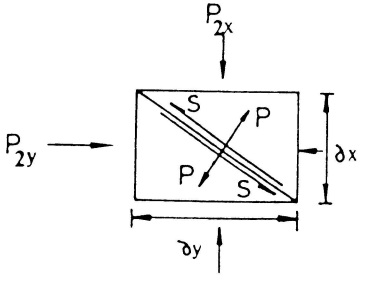

Fig. 7 (a) Enlarged Section of Element Q

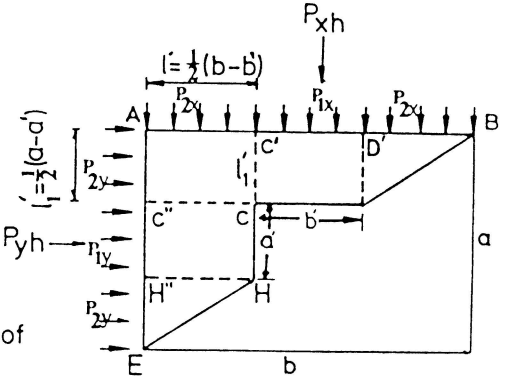

Fig. 7 (b) Load distribution along the edges

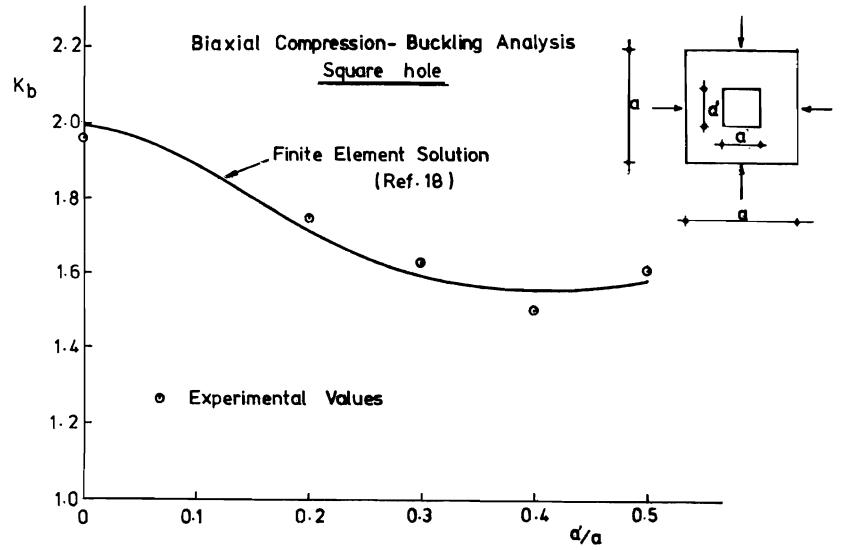
Biaxial Compression- Buckling Analysis
Square hole
Finite Element Solution
(Ref. 18)
Experimental Values
K_b
2·2
2·0
1·8
1·6
1·4
1·2
1·0
0
0·1
0·2
0·3
0·4
0·5
d/a
a
d
a
a

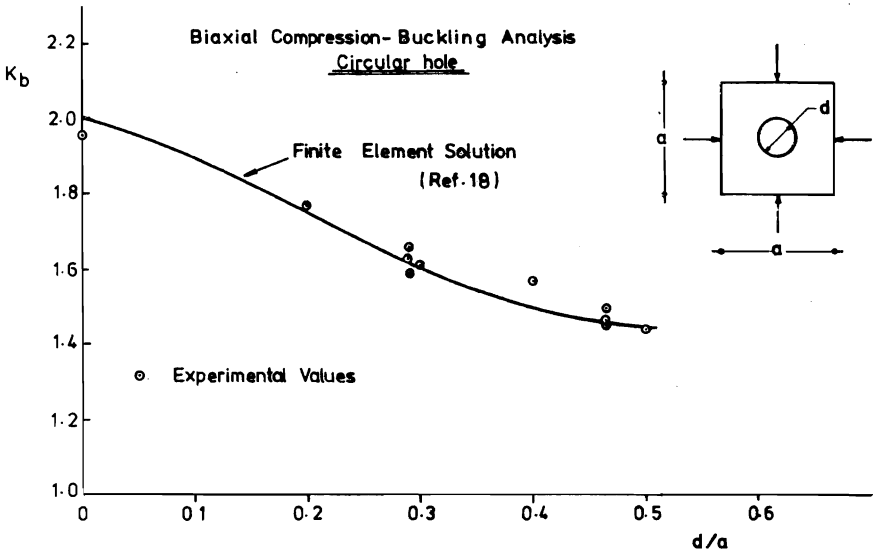
Biaxial Compression- Buckling Analysis
Circular hole
Finite Element Solution
(Ref. 18)
Experimental Values
K_b
2·2
2·0
1·8
1·6
1·4
1·2
1·0
0
0·1
0·2
0·3
0·4
0·5
0·6
d/a
a
d
a

FIGURE 8

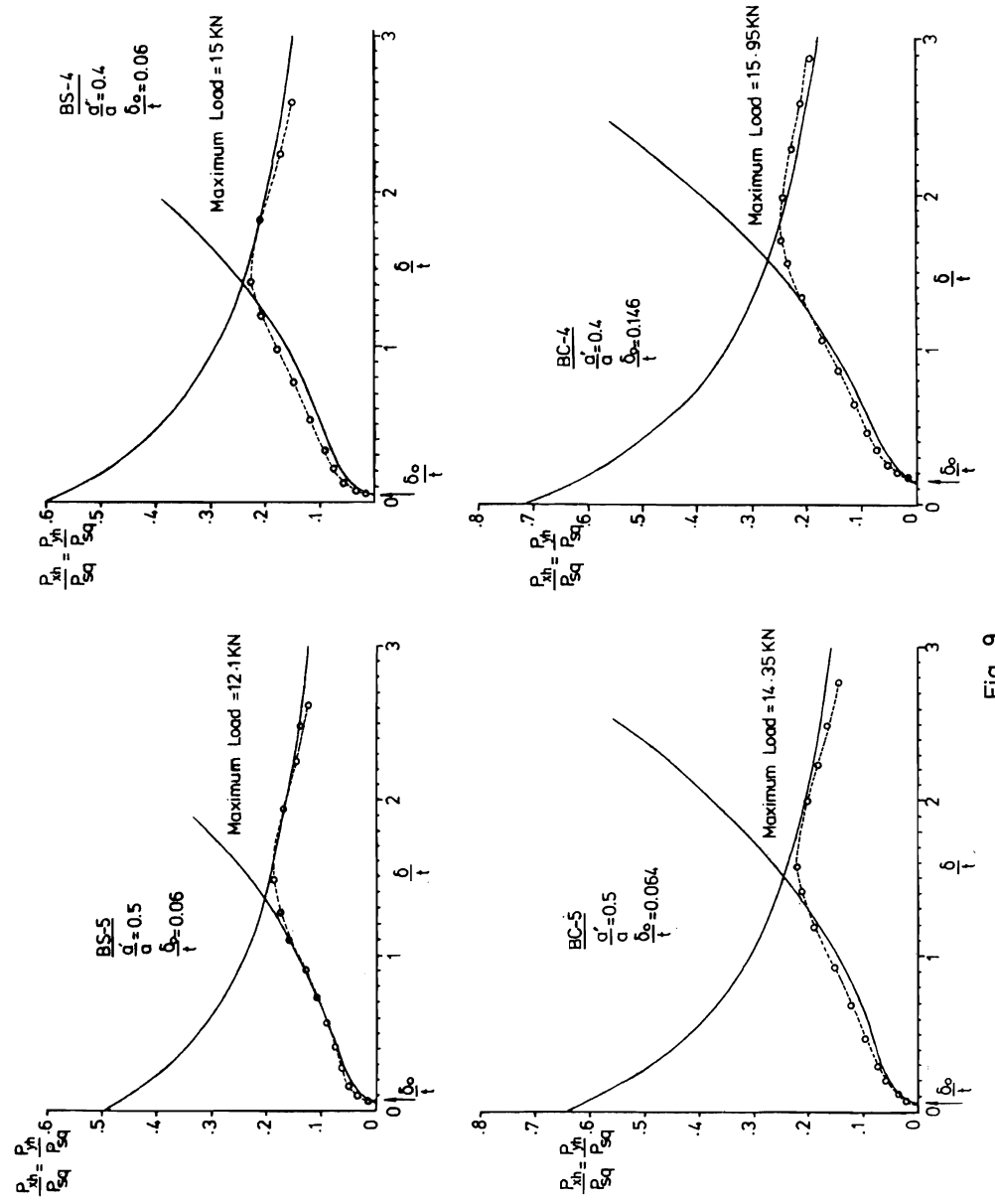
BS-4
σ'/σ=0.4
δo/t=0.06
Maximum Load = 15 KN
BC-4
σ'/σ=0.4
δo/t=0.146
Maximum Load = 15.95KN
BS-5
σ'/σ=0.5
δo/t=0.06
Maximum Load = 12.1 KN
BC-5
σ'/σ=0.5
δo/t=0.064
Maximum Load = 14.35 KN
Pxh/Psq = Pxh/Psq
δ/t
δo/t

Fig. 9

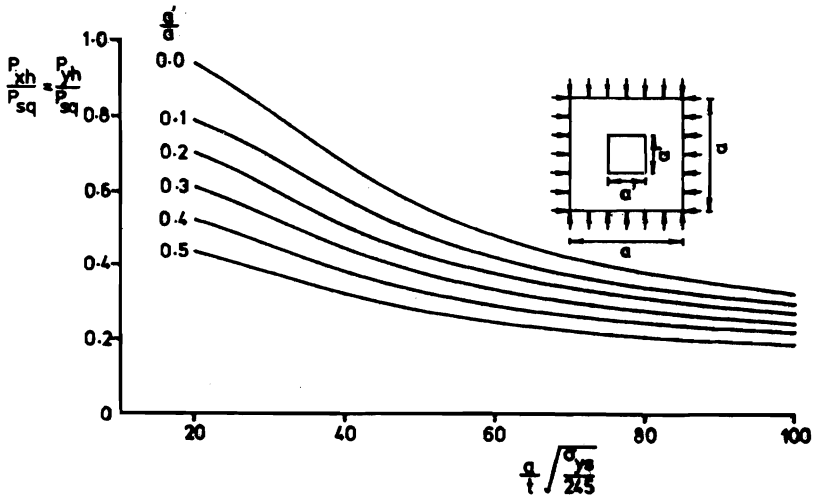

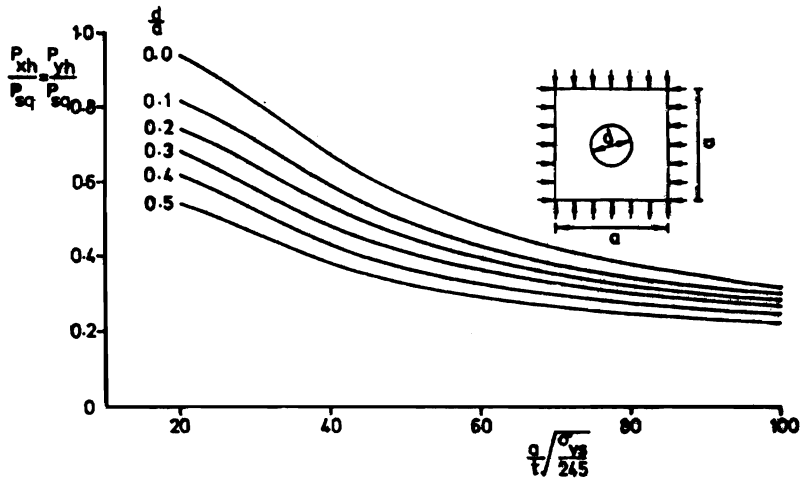

Fig. 10 DESIGN CURVES FOR BIAXIALLY LOADED PERFORATED PLATES